

Characteristics of SEPs during Solar Cycle 21-24

Raj Kumar*, Ramesh Chandra, Bimal Pande, Seema Pande

Department of Physics, DSB Campus, Kumaun University, Nainital-263001

*E-mail: rajkchanyal@gmail.com

Abstract: The study of the solar energetic particle events (SEPs) and their association with solar flares and other activities are very crucial to understand the space weather. Keeping this in view, in this paper, we present the study of the SEPs (intensity ≥ 10 pfu) during the solar cycle 21 to 24 (1976-2017) in > 10 MeV energy channels associated with solar flares. For our analysis, we have used the data from different instruments onboard SOHO satellite. We have examined the flare size, source location, CMEs characteristics of associated SEPs. About 31% and 69% of the SEPs were originated from the eastern and western solar hemisphere respectively. The average CME speed and width were 1238 km s^{-1} and 253° respectively. About 58% SEPs were associated with halo CMEs and 42% of SEPs associated with CMEs width varying from 10° to 250° respectively.

Keywords. Solar flares—solar energetic particle events—coronal mass ejections.

1. Introduction

Solar eruptions release high energetic particles, which possess the energy ranging from few tens of keV to thousands of GeV. These high energetic particles are called solar energetic particles (SEPs). These high energetic particles can reach our space-weather depending upon their location on solar surface and their direction of eruption (for detail see the review by Desai and Giacalone, 2016). If the energy of particles reaches the GeV energy range, then it is termed as ground level enhancements (GLEs).

There are two possible mechanisms responsible for the generation/origin of SEPs namely shock wave driven and magnetic reconnection. Let us discuss these mechanisms briefly as follows:

According to Reames (1999), SEPs can be generated by the shock waves driven by coronal mass ejections (CMEs). CME can generate the shock waves when the speed of CMEs is greater than the coronal sound speed. Later on many

authors confirmed it (Giacalone 2012, Reames 2012, Gopalswamy *et al.* 2015). Strong SEPs show close association with halo CMEs and the average speed of the associated CMEs are $\approx 1500 \text{ km s}^{-1}$ (Gopalswamy *et al.* 2014). Stronger shocks are driven by the high speed CMEs. Therefore, correlation between CME speed and SEP intensity should be strong. However, Gopalswamy *et al.*, (2004) found in many cases that with the occurrence of SEP event there was no corresponding type II radio burst. Solar type -II radio bursts are due to shocks generated ahead of the CMEs during eruptions. In addition to this, the correlation between CME speed and SEPs intensity is not found strong. The possible reason for this weak association was discussed in the work of Gopalswamy *et al.* 2012. According to their study this poor correlation could be due to CME-CME interaction, deflection of CMEs from the coronal hole regions etc.

Another mechanism responsible for the generation of SEPs is solar flares which are due to magnetic reconnection (Mason *et al.*, 1999,

Miteva *et al.* 2013). SEPs generated by solar flares are impulsive and short lived in nature (Cane *et al.*, 1986; Reames, 1999; Laurenza *et al.*, 2009; Cane *et al.*, 2006; Bhatt *et al.*, 2013, Chandra *et al.*, 2013). Association of the SEPs with reconnection can be confirmed by their association with type III radio bursts. If SEP events are associated with type III radio bursts it means charged particles can escape to the interplanetary space (Wild, Smerd and Weiss, 1963, Buttighoffer, 1998, Cane, Richardson and von Roseninge, 2010, Miteva *et al.*, 2014, Winter and Ledbetter, 2015, references cited therein). Authors have studied in past the SEP events with the solar X-ray flares and found a weak correlation between SEP intensity and GOES X-ray flux (Gopalswamy *et al.* 2003, Trotter *et al.* 2015).

It is believed that both the shock and flare occur during the solar eruptions. Therefore it is difficult to conclude which mechanism is responsible for the generation of SEPs.

In addition to above two discussed mechanisms, there are studies when the SEPs production depends on the properties of active region (Thalmann *et al.*, 2015, Bronarska & Michalek, 2017, Mitra *et al.*, 2018, Bruno *et al.*, 2019, Kashapova *et al.*, 2019,). These cited authors found the active regions, which are more magnetically complex produce the strong SEPs. Recently Kouloumvakos *et al.* (2015) did a statistical study of SEPs and radio type II and type III bursts. They found majority of cases were associated with both type II and III radio bursts. However, the type III radio bursts association was stronger.

From the above discussion, it is clear that the SEP production is still the subject of debate. Therefore, in this paper, we present a comparative study of SEP events (intensity ≥ 10 pfu) in > 10

MeV energy channel with the different properties of CME and GOES X-ray flares during solar cycle 21-24 (1976-2017). The paper is organized as follows: section 2 contains the description of data sets. The analysis and results are described in section 3. Section 4 presents the summary of the paper.

2. Data Sets

For the present study, we have taken the SEP events in the ≥ 10 MeV energy channel during solar cycle 21-24 (1976-2017) associated with solar flares. The proton intensity is in particle flux unit (pfu) (1 pfu is equal to $1 \text{ proton cm}^{-1} \text{ s}^{-1} \text{ sr}^{-1}$). The total number of SEP events during this period is 270. We have also counted the no. of SEPs during solar cycle 21, 22, 23 and 24. The total SEPs during 21, 22, 23 and 24 are 63, 73, 91 and 43 respectively. We have used all the observed GOES X-ray flare classes corresponding to the associated SEP events. The GOES data are downloaded from <http://sec.noaa.gov>.

We have taken the CME data from the Large Angle and Spectrometric Coronagraph (LASCO, Brueckner *et al.*, 1995) onboard Solar and Hemispheric Observatory (SOHO) satellite as cataloged at the Coordinated Data Analysis Workshops (CDAW) data center (<http://cdaw.gsfc.nasa.gov>, Gopalswamy *et al.*, 2009). The CMEs source location is taken using images and movies available at SOHO/LASCO CME catalogue ([soho/lasco cme catalogue/java movies/](http://soho.lasco.cme.catalogue/java/movies/)). Since the CME observations are available from 1997 onwards, hence the analysis before 1996 does not include the CME data. A complete table of data set used is given in the appendix.

An example of a SEP during solar cycle 24 is displayed in Figure 1. The source of this SEP is located at N14E02 on solar disc. The event was associated with a halo CME having speed $\approx 1425 \text{ km s}^{-1}$. This event is associated with GOES X1.6 class flare.

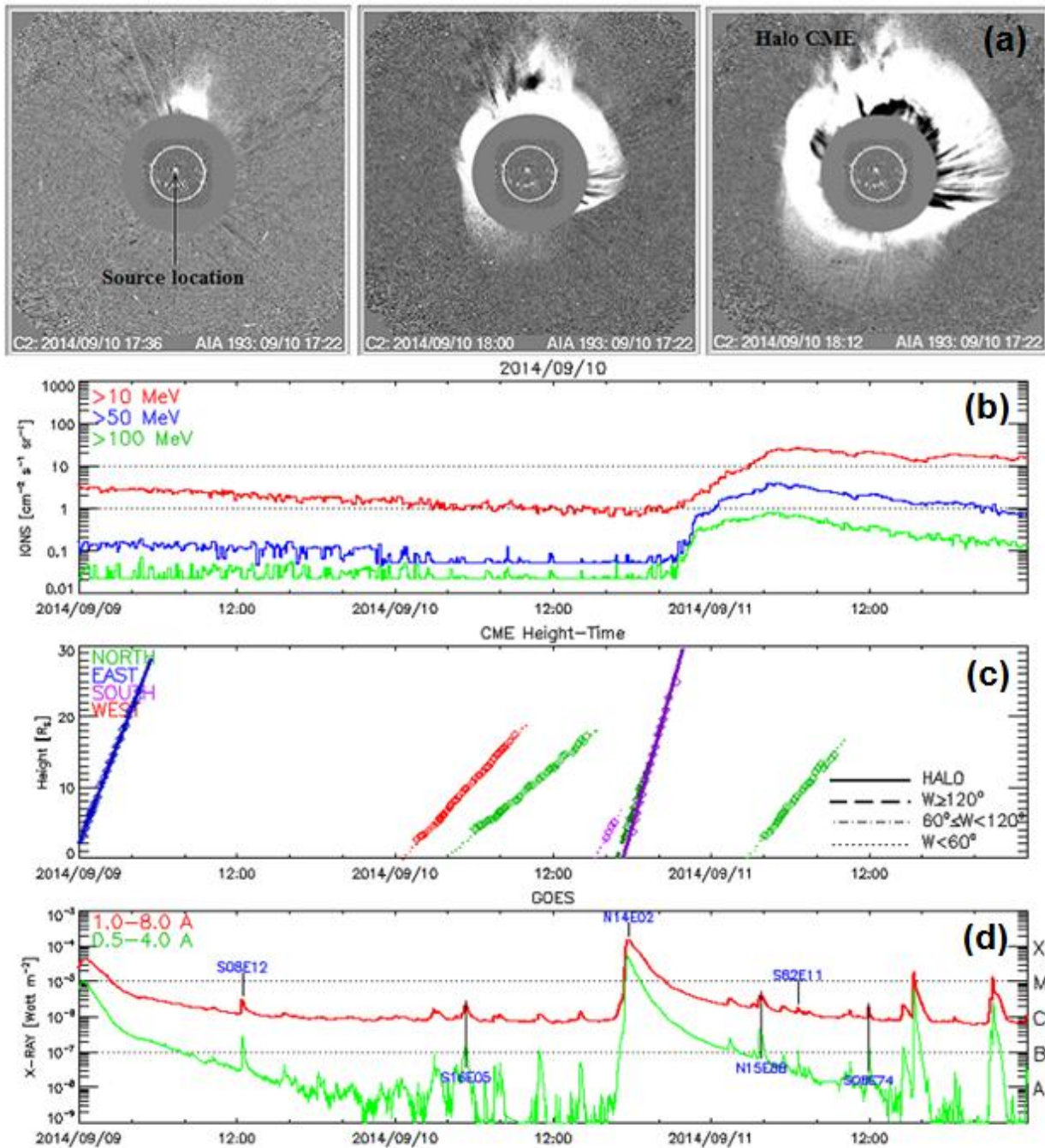


Figure 1. An example of SEP event associated with halo CME and its source region on September 10, 2014. Panel ‘a’ shows the three snap shots of halo CME that produced the SEP event. Panel ‘b’ is showing the time variation of SEP intensity in three energy channels. Panels ‘c’ and ‘d’ are showing the CME Height-Time plot and GOES soft X-ray flux in two energy channels, respectively (taken from SOHO/LASCO catalog).

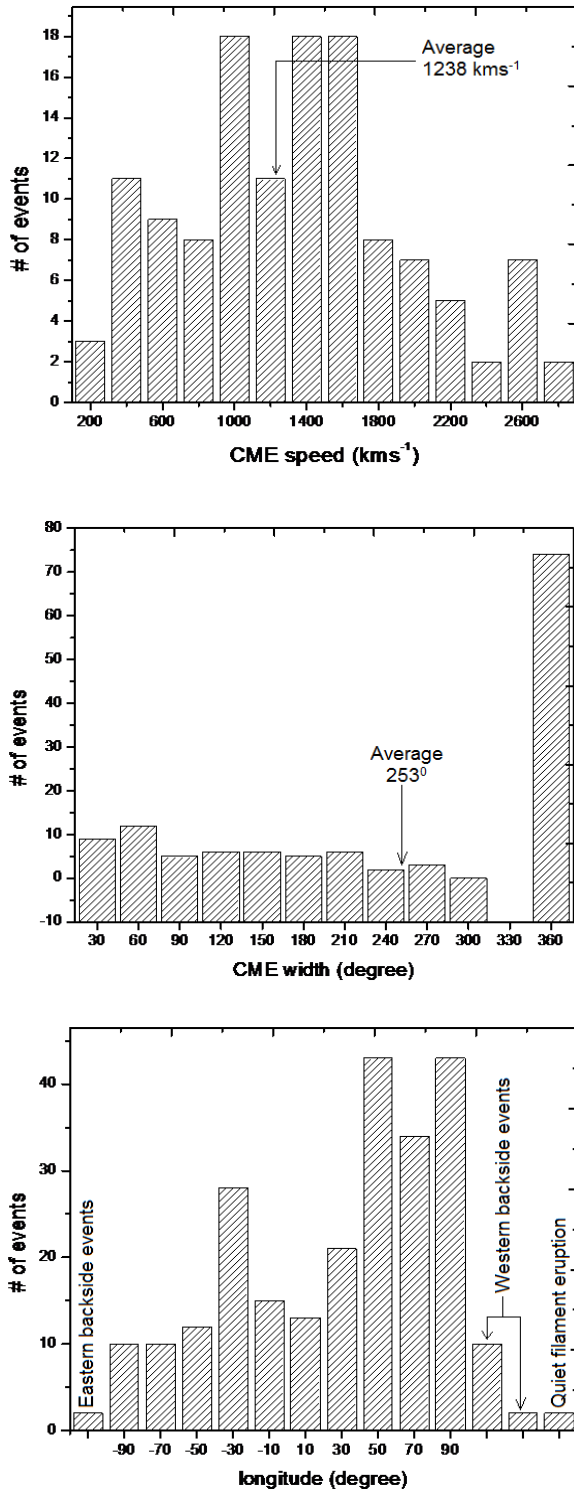


Figure 2. Histogram of number of SEP events in view of CME characteristics: Speed in kms^{-1} (top), width (middle) and source longitude (bottom).

3. Analysis and Results

Our study presents the statistical analysis of SEP events associated with solar flares during 21-24. The different statistical results are presented in following sections.

3.1 SEP events and CME characteristics

The numbers of SEP events with CME speeds is shown in Figure 2 (top). SEP events of speeds ranging from 1000 to 1600 kms^{-1} are maximum. It is about 12% of the total number of events. The average speed of the CMEs is $\approx 1238 \text{ kms}^{-1}$. About 16% of the SEPs are associated with slow CME (speed $\leq 500 \text{ kms}^{-1}$). 13% events are associated with very high speed $> 2000 \text{ kms}^{-1}$.

The variation of CMEs width and number of events is presented in the middle of the Figure 2. CME width given here is simply 2D width based on plane-of-sky observations, while the actual 3D width, in cases, could be significantly different. Jang *et al.*, 2016 did a statistical study of comparison between 2D and 3D parameters of halo CMEs. They found that the 3D widths are much smaller than the 2D widths. The average value of CME width is about 253° . The maximum number of SEP events (58%) is associated with halo CMEs. About 42% of the CMEs are distributed over the width ranging from 10° to 250° .

Figure 2 (bottom) displays the location of the sources in the eastern and western solar hemisphere. About 52% events are associated with the western solar hemisphere (longitude 20 - 90°). 23% events are originated from the central region ($\pm 20^\circ$). The region below 20° eastern solar hemisphere produced 20% events. 5% events are originated from western backside solar hemisphere and 2 events from eastern backside solar hemisphere. 2 events

are corresponding to quiet filament eruption. This is an agreement with the **scenario** that due to good magnetic connectivity most of the SEPs are originated from the western solar hemisphere.

3.2. SEP events and flare characteristics

As we have discussed in the introduction section the SEPs can be generated by the solar flares also. Therefore, we analyse here the relation between the flare class and the SEP events.

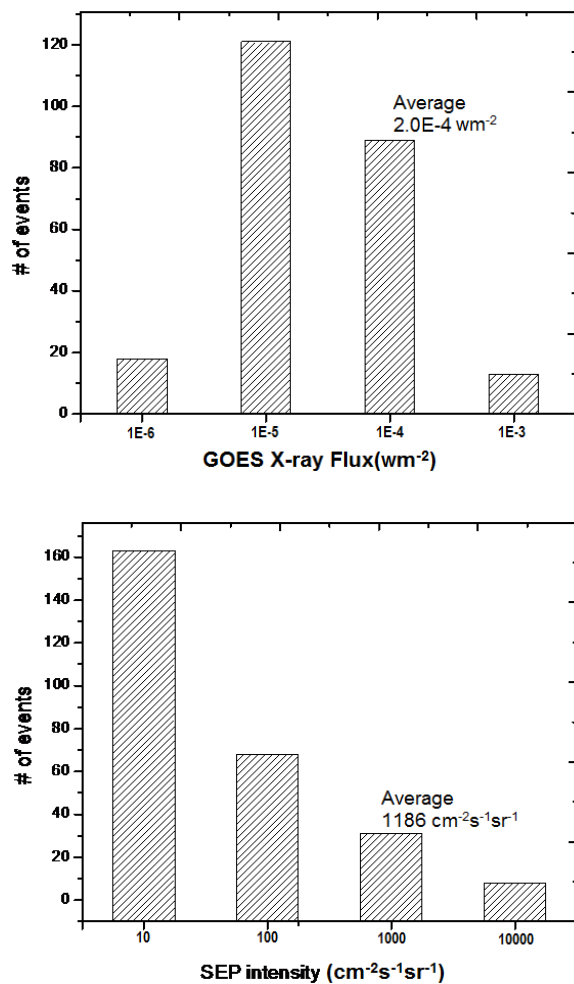


Figure 3. Histogram of number of SEP events in view of intensities: X-ray flux in Wm^{-2} (top) and SEP intensity in pfu (bottom).

Figure 3 (top) depicts the number of SEP events and the GOES X-ray flux. We observed that the average flare intensity is $2.0 \times 10^{-4} \text{ Wm}^{-2}$. We found 43% SEPs associated with X-class of solar flares. 49% and 8% SEPs are associated with M and C-class of solar flares, respectively.

SEP intensities are plotted against the number of SEP events in Figure 3 (bottom). The average SEP intensity is 1186 pfu. We have found about 60% of the SEP events have intensity 10 pfu. About 25% events have intensity between 10 to 100 pfu; 11% events in the range of 1000 pfu; events with intensity greater than 10000 pfu are 3%. It is inferred from this analysis that majority of SEPs are associated with M and X-class solar flares.

The number of C, M and X class flares is 18,121 and 102 respectively over the studies period. From solar cycle 21 to 24, number of GOES X – class flares varies as 30, 34, 27 and 11. For GOES M class, the numbers vary as 23, 32, 45 and 21 and the number of flares for GOES C class is 02, 03, 09 and 04. The occurrence rate of solar flares with solar cycles was studied in previous investigations (Howard 1974; Joshi & Pant 2005; Joshi *et al.*, 2006; Gao *et al.*, 2009; Joshi *et al.*, 2015 and references cited therein). Joshi *et al.*, 2015 found that the number of C, M and X GOES class solar flares decreased with solar cycle. However, we did not found this decreasing trend in SEP events and associated solar flares. This inconsistency indicates that all solar flares are not associated with SEP events.

3.3. Correlation analysis

In this section we have analysed the correlation of SEP intensity with CME and GOES X-ray flux. The detailed description is given in the following subsections.

3.3.1. CME speed and SEP intensity

Figure 4 presents the scatter plot between CMEs speed and SEP intensity. We compute the correlation coefficient between these two parameters and the value is 0.39.

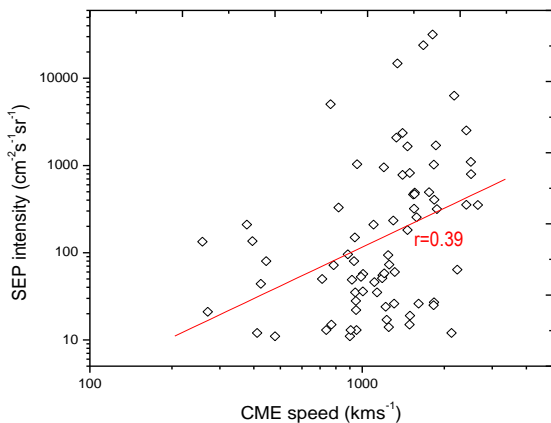


Figure 4. Scatter plot between CME speed and SEP intensity for all events.

This indicates the weaker correlation between these quantities. Further we have calculated the correlation coefficient for the longitude range i.e., eastern (20 to 70°), central ($\pm 20^{\circ}$) and western (20 to 70 and 70 to 90°). For our analysis, we have not considered the events originating from eastern hemisphere from longitude 70 to 90° , because we found only four events within this longitude range. The results are presented in Figure 5. The correlation coefficient for longitude range from 20 to 70° in eastern hemisphere is 0.41. The correlation coefficient is 0.52 for the

central region. As we move in the western hemisphere from the longitude 20 to 70° , the correlation coefficient becomes poor with value 0.38. From longitude range 70 to western limb the correlation becomes maximum i.e., 0.53. This confirms the idea that when we move towards western limb, the magnetic connectivity becomes better as proposed in Parker spiraling. Our this result is in agreement with the previous findings (Kahler, 2001; Gopalswamy *et al.*, 2003, 2004 and references therein).

3.3.2. Flare class and SEP intensity

The correlation between X-ray flare flux and SEPs intensity is presented in Figure 6. The top panel of figure presents plot for the events associated with all CMEs (including total CMEs width), while the bottom panel shows the plot for the events, which are associated with halo CMEs. The correlation coefficient for the total and the events associated with halo CMEs are 0.40 and 0.34 respectively. However, in both the cases, the correlation coefficient is poor, which support the earlier studies (Gopalswamy *et al.*, 2003, 2004, Chandra *et al.*, 2013). Moreover, we observed that the correlation coefficient is decreased when we took only halo CMEs. This decrease in correlation may be explained by the fact that during the halo CMEs the contribution from the shock is dominated in comparison to the solar flares. Another possibility for this poor correlation could be the weak acceleration of particles during the flare time. Due to this weak acceleration the charged particles cannot reach the interplanetary space.

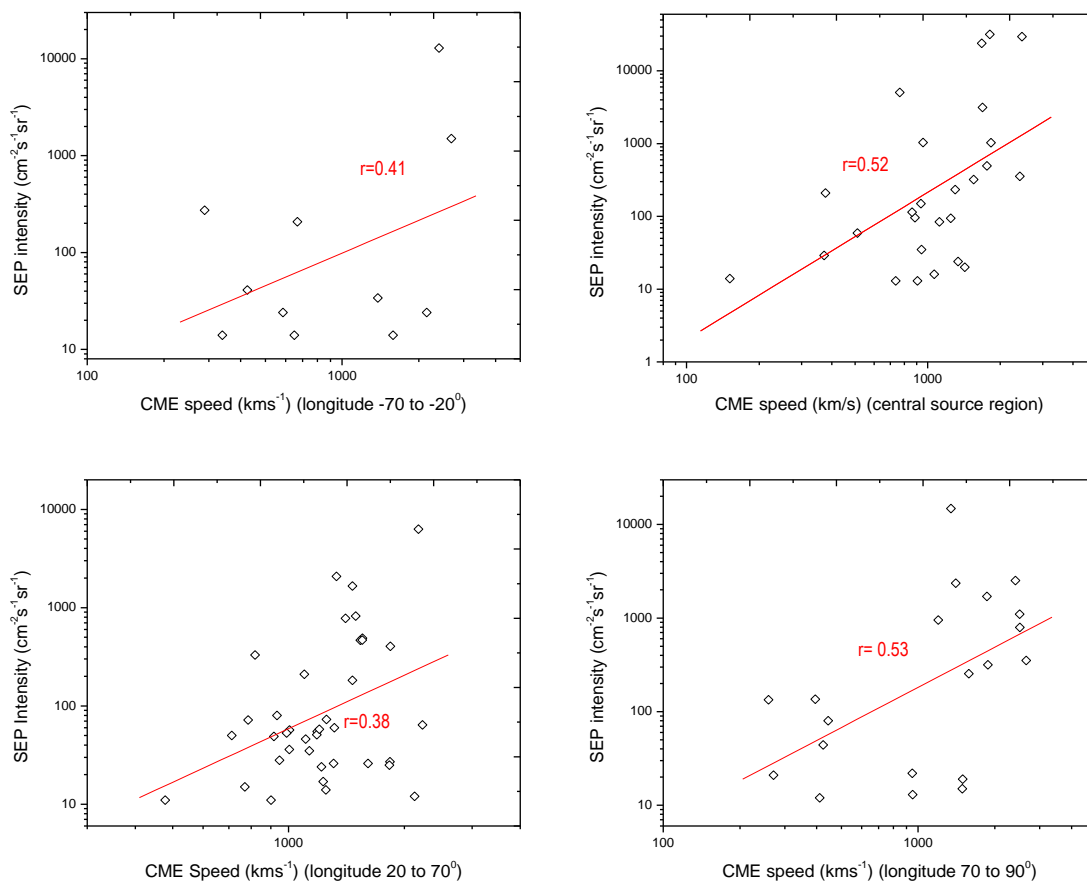


Figure 5. Scatter plots between SEP intensity and CME speed for different longitude zones of solar surface. Central zone is defined as the longitude $\pm 20^\circ$. The regression line and correlation coefficients (r) are shown in plots.

3.4 GLEs during Solar Cycle 23 and 24

We have selected some events from solar cycle 23 and 24, which produced ground level enhancements (GLEs) listed at <http://gle.oulu.fi> site. We chose this period of events because of the availability of LASCO CME data. This is given in Table 1. We examined the properties/characteristics of these GLE associated parameters. We found the majority of GLEs (77%) were associated with halo CMEs. The speed of all the associated CMEs was high ranging from 938

to 2598 km s^{-1} . For one event (August 24, 1998) the CME data was not available. 10 out of 13 associated flares were X-class and 02 were M-class flares. One event was not associated with any GOES X-ray flare. It was produced by filament eruption. However, the speed of associated CME was very high i.e. 2465 km s^{-1} . This speed indicates the production of strong shock during the CME propagation. All these GLE producing event sources were located either in central region or close to western limb. The properties of GLE events were discussed in detail by Gopalswamy *et al.* 2012. Richardson and

Cane (2010) also made a study, which summarized different properties of the ICME during the solar cycle 23.

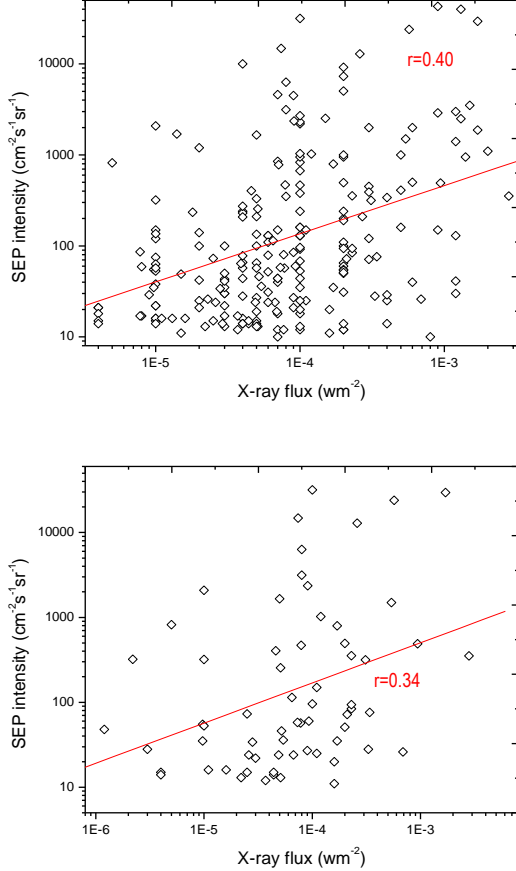


Figure 6. Scatter plots between X-ray peak flux and SEP intensity (top) and same plot for the events associated with halo CMEs (bottom). The regression line and correlation coefficients are also shown in figure.

4. Summary

In this paper we have studied the SEP events associated with solar X-ray flares and CMEs. For this study, a large data was taken from solar cycle 21 to 24.

We have studied the flare size, CME speed, CME width, source location with the

number of SEP events and SEP intensity. The main results are summarized as follows:

- Average CME speed over that large period of data comes to be 1238 km s^{-1} . Maximum number of SEP events has the CME speed between 1000 km s^{-1} to 1600 km s^{-1} .
- Average CME width is 253 degree i.e., maximum of the SEP events are associated with halo CMEs and partial halo ($> 120^\circ$) CMEs. This result confirms the previous findings that wider CMEs can produce more strong SEPs.
- Majority of SEP producing solar flares are GOES M and X-class.
- The correlation study of SEP and CME speed shows the value of correlation coefficient is 0.41 in eastern hemisphere ($> 20^\circ$ east). When we move towards the western hemisphere the coefficient becomes stronger (0.52 to 0.53). The correlation between SEP intensity and X-ray flux is found 0.40 . It becomes rather poor when we take the events associated with halo CMEs only. Correlation reduces to 0.34 .
- The GLE events during solar cycle 23 & 24 are associated with major flares and high speed CMEs.
- This study is interesting to demonstrate how the forecast using the characteristics of CMEs cannot be done with a better rate than 50% . Progresses on the fundamental physics should be done before having a more precise forecast.

From our analysis, we have found neither the flare intensity nor the CME speed are tightly correlated with the SEP intensity. For the better understanding of SEPs, we need to consider the magnetic topology of the active

Table 1. SEP events of solar cycle 23 & 24 associated with GLE.

Date	CME speed	CME width	Source location	Flare class	SEP intensity
06-11-97	1556	H	S18W63	X9.4	490
02-05-98	938	H	S15W15	X1.1	150
06-05-98	1099	190	S11W65	X2.7	210
24-08-98	No CME data		N30E07	X1.0	670
14-07-00	1674	H	N22W07	X5.7	24000
15-04-01	1199	167	S20W85	X14	951
18-04-01	2465	H	S23W92	Filament eruption	321
04-11-01	1810	H	N06W18	X1.0	31700
26-12-01	1446	212	N08W54	M7.1	779
24-08-02	1878	H	S02W81	X3.1	317
28-10-03	2459	H	S16E08	X17	29500
02-11-03	2598	H	S14W56	X8.3	1570
17-05-12	1582	H	N11W76	M5.1	255

regions together with the CME and flare characteristics.

Here, we would like to mention that the big uncertainty due to the measurement at L1 (a single point) limits the statistical analysis. For the better statistical results, we need an armada of spacecraft to have a better view of the solar wind. Parker solar probe and Solar Orbiter will bring certainly important information.

Acknowledgements

We would like to thank the reviewers for their constructive and important suggestions, which improve the paper considerably. We acknowledge the open data policy of NGDC, SOHO and SDO. RC acknowledges the support from SERB-DST project no. SERB/F/7455/2017-17.

References

Bhatt, N.J., Jain, R., Awasthi, A.K., 2013, Res. Astron. Astrophys. 13, 978–990.

- Bronarska, K., Michalek, G., 2017, Advances in Space Research, 59 (1), 384-392.
- Brueckner, G.E., Howard, R.A., Koomen, D.J., *et al.*, 1995, Sol. Phys., 162, 357–402.
- Bruno, A., Christian, E.R., Nolfo, G.A. de, *et al.*, 2017, Space Weather, 17, 419–437.
- Buttighoffer, A., 1998, A & A, 335, 295-302.
- Cane, H.V., McGuire, R.E., von Roseninge, T.T., 1986, Ap J. 301, 448–459.
- Cane, H.V., Mewaldt, R.A., Cohen, C.M.S., von Roseninge, T.T., 2006, J. Geophys. Res. 111, A06S90.
- Cane, H. V., Richardson, I. G., von Roseninge, T. T., 2010, J. Geophys. Res. 115, A08101.
- Chandra, R., Gopalswamy, N., Makela, P., *et al.*, 2013, Adv. Sp. Res., 52, 2102-2111.
- Desai, M. and Giacalone, J., 2016, Living Rev. Sol. Phys.13:3, 1-132.
- Gao, P.X., Li, K.J., & Shi, X.J. 2009, MNRAS, 400, 1383.
- Giacalone, J., 2012, ApJ, 761 (1), 28-39.
- Gopalswamy, N., Yashiro, S., Lara, A., *et al.*, 2003, J. Geophys. Res. Lett. 30(12), 8015.

- Gopalswamy, N., Yashiro, S., Krucker, S., Stenborg, G., Howard, R.A., 2004, *J. Geophys. Res.* 109, A12015.
- Gopalswamy, N., Xie, H., Yashiro, S., *et al.*, 2012, *Space Science Rev.*, 171, 23-60.
- Gopalswamy, N., Xie, H., Akiyama, S., *et al.*, 2014, *Earth, Planets and Space*, 66,104-118.
- Gopalswamy, N., Makela, P., Akiyama, S., *et al.*, 2015, *Sun and Geosphere*, 10 (2), 111-118.
- Howard, R. 1974, *Sol. Phys.*, 38, 59.
- Jang, S., Moon, Y. J., Kim, R.S., *et al.*, 2016, *APJL*, 821:95 (8pp).
- Joshi, B., Bhattacharyya, R., Pandey, K., K., *et al.*, 2015, *A&A* 582, A4 (2015).
- Joshi, B., & Pant, P. 2005, *A&A*, 431, 359.
- Joshi, B., Pant, P., & Manoharan, P. K. 2006, *JA&A*, 27, 151.
- Kahler, S.W., 2001, *J. Geophys. Res.* 106, 20947–20956.
- Kashapova, L. K., Miteva, R., Myagkova, I. N., *et al.*, 2019, *Sol. Phys.*, 294 (1), 9-24.
- Kouloumvakos, A., Nindos, A., Valtonen, E., *et al.*, 2015, *A&A*, 580, 80-96.
- Laurenza, M., Cliver, E.W., Hewitt, J., *et al.*, 2009, *Space Weather*, 7 (4), 1-18.
- Mason, G.M., Mazur, J.E., Dwyer, J.R., 1999, *ApJL*, 525, 133–136.
- Miteva, R., Klein, K.-L., Malandraki, O., Dorrian, G., 2013, *Sol. Phys.*, 282, 579 - 613.
- Miteva, R., Klein, K.-L., Kienreich, I., *et al.*, 2014, *Sol. Phys.*, 289 (7), 2601-2631.
- Mitra, P.K., Joshi, B., Prasad, A., *et al.*, 2018, *APJL*, 869, 69-87.
- Reames, D. V., 1999, *Space Sci. Rev.* 90, 413-491.
- Reames, Donald V., 2012, *ApJ*, 757(1), 93-100.
- Richardson, I. G., Cane, H. V., 2010, *Sol. Phys.*, 264 (1), 189-237.
- Thalmann, J. K., Su, Y., Temmer, M., *et al.*, 2015, *ApJL*, 801 (2), 23-27.
- Trottet, G., Samwel, S., Klein, K., -L. *et al.* 2015, *Sol. Phys.*, 290, 819-839.
- Wild, J. P., Smerd, S. F., Weiss, A. A., 1963, *Annual Review of Astronomy and Astrophysics*, 1, 291-366.
- Winter, L. M., Ledbetter, K., 2015, *ApJ.*, 809, 105-123.

Appendix (Data set)

SEP		CME			Source Location	Active Region No.	Flare Class	SEP Intensity(pfu)
Date	Time	Time	Speed	Width				
Data from 1976 to 1996								
30-04-76	21:20	No CME Observation during 1976- 1996	S09W47	700	X2	12		
19-09-77	14:30		N08W58	889	X2	200		
22-11-77	14:00		N24W38	939	X1	160		
13-02-78	9:30		N22W13	1001	M7	850		
11-04-78	15:30		N19W54	1057	X2	65		
29-04-78	4:45		N22E41	1092	X5	1000		
07-05-78	4:20		N22W64	1095	X2	100		
02-06-78	7:30		N23W50	1129	M5	19		
24-06-78	9:00		N19E18	1164	M2	25		
13-07-78	3:00		NO FLARE				20	
23-09-78	10:35		N35W50	1294	X1	2200		
10-11-78	21:30		N17E02	1385	M1	38		
17-02-79	20:20		N15E48	1574	X2	31		
03-04-79	16:00		NO FLARE				45	
06-06-79	18:50		N20E16	1781	X2	950		
07-07-79	0:15		NO FLARE				50	
19-08-79	8:50		N10E90	1943	X6	500		
15-09-79	15:00		N10E90	1994	X2	60		
16-11-79	4:30		N34W25	2110	M1	75		
06-02-80	13:40		NO FLARE				12	
17-07-80	23:00		S12E06	2562	M3	100		
30-03-81	9:00		N13W74	2993	M3	30		
10-04-81	17:45		N09W40	3025	X2	50		
24-04-81	15:15		N18W50	3049	X5	160		
09-05-81	12:00		N09E37	3099	M7	150		
15-05-81	3:00		N11E58	3106	X1	130		
20-07-81	14:30		S26W75	3204	M5	100		
25-07-81	6:00		NO FLARE				18	
10-08-81	1:15		S10E24	3257	M4	57		
08-10-81	12:35		S19E88	3390	X3	2000		
10-12-81	5:45		N12W16	3496	M5	65		
31-10-82	0:55		S13E19	3576	X1	830		
06-06-82	2:45		S09E72	3763	X8	10		
09-06-82	0:40		S11E26	3763	X12	30		
11-07-82	7:00		N17E73	3804	X9	2900		

22-07-82	20:30		N29W86	3804	M4	240
05-09-82	22:05		N11E30	3886	M4	66
22-11-82	19:40		S11W43	3994	M7	40
26-11-82	6:05		S11W87	3994	X4	25
08-12-82	0:10		S14W81	4007	X2	1000
17-12-82	18:45		S10E24	4026	X12	130
19-12-82	19:20		N10W75	4022	M9	85
27-12-82	6:00		S14E31	4033	X2	190
03-02-83	12:00		S19W08	4077	X4	340
15-06-83	4:35		S09W90	4201	NO FLARE	18
16-02-84	9:15		S12W90	4408		660
19-02-84	13:10		N16E82	4421	X2	55
13-03-84	14:40		NO FLARE			10
14-03-84	4:05		S12W42	4433	M2	100
25-04-84	13:30		S12E43	4474	X13	2500
24-05-84	10:45		S09E24	4492	M6	31
31-05-84	13:15		S08W38	4492	M1	15
22-01-85	4:15		N01W76	4617	X4	14
25-04-85	14:30		N02E01	4647	X1	160
09-07-85	2:35		S16W36	4671	M2	140
06-02-86	9:25		S04W06	4711	X1	130
14-02-86	11:55		N01W76	4713	M6	130
06-03-86	18:35		N02E01	4717	C4	21
04-05-86	12:55		N06W90	4717	M1	16
06-02-86	9:25		S04W06	4711	X1	130
14-02-86	11:55		N01W76	4713	M6	130
06-03-86	18:35		N02E01	4717	C4	21
04-05-86	12:55		N06W90	4717	M1	16
08-11-87	2:00		N31W90	4875	M1	120
02-01-88	23:25		S34W18	4912	X1	92
25-03-88	22:25		N22W90	4965	NO FLARE	58
30-06-88	10:55		S16E22	5060		21
26-08-88	0:00		N24E90	5125	M2	42
12-10-88	9:20		S20W66	5175	X2	12
08-11-88	22:25		S17W47	5212	M3	13
14-11-88	1:30		S23W27	5227	M3	13
17-12-88	6:10		N27E59	5278	X1	18
17-12-88	20:00		N26E37	5278	X4	29
04-01-89	23:05		S20W60	5303	M4	28
08-03-89	17:35		N35E69	5395	X15	3500
17-03-89	18:55		N33W60	5395	X6	2000

23-03-89	20:40		N18W28	5409	X1	53
11-04-89	14:35		N35E29	5441	X3	450
05-05-89	9:05		S20W36	5464	M5	27
06-05-89	2:35		N30E01	5470	X2	110
23-05-89	11:35		N20W35	5477	X1	68
24-05-89	7:30		S21E16	5497	M5	15
18-06-89	16:50		N12W31	5534	C4	18
30-06-89	6:55		N26W60	5555	M3	17
01-07-89	6:55		N11E20	5590	M3	17
25-07-89	9:00		N25W84	5603	X2	54
12-08-89	16:00		S16W37	5629	X2	9200
04-09-89	1:20		S18E16	5669	X1	44
12-09-89	19:35		S18W79	5669	M5	57
29-09-89	12:05		S26W90	5698	X9	4500
06-10-89	0:50		S20E12	5710	X1	22
19-10-89	13:05		S27E10	5747	X13	40000
09-11-89	2:40		N18W50	5155	M3	43
15-11-89	7:35		N11W26	5786	X3	71
27-11-89	20:00		N30E05	5800	X1	380
30-11-89	13:45		N26W59	5800	X2	7300
19-03-90	7:05		N31W43	5969	X1	950
29-03-90	9:15		S04W37	5988	M4	16
07-04-90	22:40		N22E72	6007	M7	18
11-04-90	21:20		N21W24	6013	C3	13
17-04-90	5:00		N32E57	6022	X1	12
28-04-90	10:05		S40W13	6050	M1	150
21-05-90	23:55		N35W36	6063	X5	410
24-05-90	21:25		N33W78	6063	X9	150
28-05-90	7:15		NO FLARE			45
12-06-90	11:40		N10W33	6089	M6	79
26-07-90	17:20		NO FLARE			21
01-08-90	0:05		N20E45	6180	M4	230
30-01-91	11:30		S17W35	6469	X1	240
25-02-91	12:10		S16W80	6497	X1	13
23-03-91	8:20		S26E28	6555	X9	43000
29-03-91	21:20		N19W50	6560	X1	20
03-04-91	8:15		N14W00	6562	M6	52
13-05-91	3:00		S09W90	6615	M8	350
31-05-91	12:25		NO FLARE			22
04-06-91	8:20		N30E70	6659	X12	3000
14-06-91	23:40		N33W69	6659	X12	1400

30-06-91	7:55				N30E85	6703	M6	110
07-07-91	4:55				N26E03	6703	X1	2300
11-07-91	2:40				S22E34	6718	M3	30
11-07-91	22:55				N30W44	6770	X2	14
26-08-91	17:40				N25E64	6805	X2	240
01-10-91	17:40				S21E32	6853	M7	12
28-10-91	13:00				S13E15	6891	X6	40
30-10-91	7:45				S08W25	6891	X2	94
07-02-92	6:45				S13W10	7042	M4	78
16-03-92	8:40				S14E29	7100	M7	10
09-05-92	10:05				S26E08	7154	M7	4600
25-06-92	20:45				N09W67	7205	X3	390
06-08-92	11:45				S09E68	7248	M4	14
30-10-92	19:20				S22W61	7321	X1	2700
04-03-93	15:05				S14W56	7434	C8	17
12-03-93	20:10				S00W51	7440	M7	44
20-02-94	3:00				N09W02	7671	M4	10000
20-10-94	0:30				N12W24	7790	M3	35
20-10-95	8:20				S09W55	7912	M1	63
Data from 1977 to 2017, where CME data is available								
04-11-97	7:00	6:10	785	H	S14W33	8100	X2.1	72
06-11-97	13:00	12:10	1556	H	S18W63	8100	X9.4	490
20-04-98	11:00	10:07	1863	165	S43W90	-	M1.4	1700
02-05-98	14:00	14:06	938	H	S15W15	8210	X1.1	150
06-05-98	8:00	8:29	1099	190	S11W65	8210	X2.7	210
09-05-98	5:00	3:35	2331	178	>SW90	8210	M7.7	12
24-08-98	23:55	NO DATA			N30E07	8307	X1	670
25-09-98	0:10				N18E09	8340	M7	44
30-09-98	15:20				N23W81	8340	M2	1200
08-11-98	2:45	1:25	350	20	NO FLARE			11
14-11-98	8:10	NO DATA			N28W90	8375	C1	310
23-01-99	11:05				N27E90	-	M5	14
24-04-99	15:00	13:31	1495	H	>NW90	No Flare		32
03-05-99	13:00	6:06	1584	H	N15E32	8530	M4.4	14
05-05-99	18:20	16:26	649	42	N15E32	8525	M4	14
01-06-99	20:00	19:37	1772	H	>NW90	-	C1.2	48
02-06-99	2:45	4:50	422	39	NO FLARE			48
04-06-99	8:00	7:26	2230	150	N17W69	8552	M3.9	64
18-02-00	10:00	9:54	890	118	>NW90	NO FLARE		13
04-04-00	17:00	16:32	1188	H	N16W66	8933	C9.7	55
06-06-00	19:00	15:54	1119	H	N20E18	9026	X2.3	84

10-06-00	18:00	17:08	1108	H	N22W38	9026	M5.2	46
14-07-00	11:00	10:54	1674	H	N22W07	9077	X5.7	24000
22-07-00	12:00	11:54	1230	105	N14W56	9085	M3.7	17
28-07-00	10:50	16:54	394	9	NO FLARE			18
11-08-00	16:50	16:54	300	35	NO FLARE			17
12-09-00	13:00	11:54	1550	H	S17W09	9163	M1	320
16-10-00	8:00	7:27	1336	H	>W90	9193	M2.5	15
25-10-00	12:00	8:26	770	H	N10W66	9199	C4	15
08-11-00	23:00	23:06	1345	H	N10W77	9213	M7.4	14800
24-11-00	14:00	15:30	1245	H	N22W07	9230	X2.3	94
28-01-01	17:00	15:54	916	250	S04W59	9313	M1.5	49
29-03-01	11:00	10:26	942	H	N20W19	9393	X1.7	35
02-04-01	23:00	22:06	2505	244	N19W72	9390	X20	1100
10-04-01	8:00	5:30	2411	H	S23W09	9415	X2.3	355
12-04-01	12:00	10:31	1184	H	S19W43	9415	X2	51
15-04-01	14:00	14:06	1199	167	S20W85	9415	X14	951
18-04-01	3:00	2:30	2465	H	S23W92	9424	C2.2	321
28-04-01	14:00	12:30	1006	H	N17W31	9433	M7.8	57
07-05-01	13:00	12:06	1223	205	>NW90	NO FLARE		30
15-06-01	16:00	15:56	1701	H	>SW90	NO FLARE		26
09-08-01	19:00	NO DATA			S17E19	9570	C7.8	17
16-08-01	1:00	23:54	1575	H	Backside	NO FLARE		493
15-09-01	2:00	11:54	478	130	S21W49	9608	M1.5	11
24-09-01	11:00	10:30	2402	H	S16E23	9632	X2.6	12900
01-10-01	13:00	5:30	1405	H	S20W84	9628	M9.1	2360
19-10-01	17:30	16:50	901	H	N15W29	9661	X1.6	11
22-10-01	17:00	15:06	1336	H	S21E18	9672	M6.7	24
04-11-01	17:00	16:35	1810	H	N06W18	9684	X1	31700
17-11-01	6:00	5:30	1380	H	S13E42	9704	M2.8	34
22-11-01	21:00	20:30	1443	H	S25W67	9704	M3.8	
22-11-01	24:00:00	23:30	1437	H	S15W34	9704	M9.9	
26-12-01	5:30	5:30	1406	212	N08W54	9742	M7.1	779
29-12-01	24:00:00	20:06	2044	H	S26E90	9756	X3.4	76
08-01-02	3:00	17:54	1794	H	>NE90	NO FLARE		91
14-01-02	24:00:00	5:35	1492	H	S28W83	-	M4.4	15
20-02-02	6:00	6:30	952	H	N12W72	9825	M5.1	13
15-03-02	3:00	23:06	907	H	S08W03	9866	M2.2	13
18-03-02	6:00	2:54	989	H	S09W46	9866	M1	53
22-03-02	13:30	11:06	1750	H	>SW90	9986	M1.6	16
17-04-02	10:30	8:26	1218	H	S14W34	9906	M2.6	24
21-04-02	2:30	1:27	2409	241	S14W84	9906	X1.5	2520

22-05-02	6:00	3:50	1494	H	S30W34	-	C5	820
07-07-02	13:00	11:06	1329	>205	>W90	17	M1	22
15-07-02	10:30	21:30	1300	>188	N19W01	30	M1.8	234
20-07-02	6:00	21:30	2017	H	>SE90	39	X3.3	28
14-08-02	3:00	2:30	1309	133	N09W54	61	M2.3	26
22-08-02	2:30	2:06	1005	H	S07W62	69	M5.4	36
24-08-02	1:30	1:27	1878	H	S02W81	69	X3.1	317
07-09-02	4:40	3:54	668	66	N09E28	102	M4	208
09-11-02	15:00	13:31	1838	H	S12W29	180	M4.6	404
28-05-03	23:35	00:50	1366	H	S07W17	365	X3	121
31-05-03	4:40	2:30	1835	H	S07W65	365	M9	27
18-06-03	20:50	13:31	586	135	S08E61	386	M6	24
26-10-03	18:25	17:54	1537	171	N02W38	484	X1	466
28-10-03	12:15	11:30	2459	H	S16E08	486	X17	29500
02-11-03	11:05	11:30	826	33	NO FLARE			1570
04-11-03	22:25	19:54	2657	H	S19W83	486	X28	353
21-11-03	23:55	19:27	737	82	N02W17	501	M5	13
02-12-03	15:05	10:50	1393	150	W limb	-	C7.8	86
11-04-04	11:35	11:54	1132	H	S14W47	588	C9.7	35
25-07-04	18:55	14:54	1333	H	N08W33	652	M1	2086
13-09-04	21:05	20:48	289	47	N04E42	672	M4	273
19-09-04	19:25	22:18	-	99	N03W58	672	M1	57
01-11-04	6:55	6:06	925	146	Backside	NO FLARE		63
07-11-04	19:10	16:54	1759	H	N09W17	696	X2	495
16-01-05	2:10	5:30	765	31	N15W05	720	X2	5040
14-05-05	5:25	17:12	1689	H	N12E11	759	M8	3140
16-06-05	22:00	13:36	424	85	N09W87	775	M4	44
14-07-05	2:45	3:54	259	25	N10W80	786	M5	134
27-07-05	23:00	23:54	246	21	N11E90	792	M3	41
22-08-05	20:40	22:30	819	57	S12W60	798	M5	330
08-09-05	2:15	No Data			S06E89	808	X17	1880
14-08-10	12:30	10:12	1250	H	N17W52	1099	C4	14
07-03-11	21:50	20:00	2125	H	N30W47	1164	M3.7	12
08-03-11	1:05	20:15	712	99	N24W59	1164	M3	50
21-03-11	19:50	2:24	1341	H	Backside	1169	NO FLARE	14
07-06-11	8:20	6:49	1255	H	S21W54	1226	M2.5	73
04-08-11	5:16	4:12	1315	H	N19W36	1261	M9.3	60
09-08-11	8:45	8:12	1610	H	N17W69	1263	X6.9	26
23-09-11	22:55	0:48	1116	44	N11E74	1302	X1/2N	35
26-11-11	11:25	7:12	933	H	N08W49	1353	NO FLARE	80
23-01-12	5:30	4:00	2175	H	N28W36	1402	M8	6310

27-01-12	18:55	18:27	2508	H	N27W71	1402	X1.7	795
07-03-12	2:50	0:24	2684	H	N17E27	1429	X5.4	1500
13-03-12	18:05	17:36	1554	H	N17W66	1429	M7.9	469
17-05-12	1:55	1:48	1582	H	N11W76	1476	M5.1	255
27-05-12	5:35	5:48	725	197	NO FLARE			14
16-06-12	19:55	15:48	151.00	10	S17E14	1504	M1	14
06-07-12	5:00	23:24	1828	H	S13W59	1515	X1.1	25
07-07-12	4:00	4:48	9	195	S18W50	1515	X1	25
08-07-12	18:10	16:54	1495	157	S17W74	1515	M6.9	19
12-07-12	18:35	16:48	885	H	S16W09	1520	X1	96
17-07-12	17:15	17:00	395	96	S17W75	1520	M1	136
19-07-12	6:40	4:24	444	11	S13W88	1520	M7.7	80
23-07-12	15:45	17:48	411	27	S16W86	1520	NO FLARE	12
01-09-12	13:35	13:36	511	35	S06E20	-	C8	59
28-09-12	3:00	0:12	947	H	N08W41	1577	C3	28
15-03-13	19:40	7:12	1063	H	N11E12	1692	M1.1	16
11-04-13	8:25	7:24	861	H	N09E12	1719	M6.5	114
14-05-13	13:25	12:36	425	10	N11E51	1748	X12	41
22-05-13	14:20	13:25	1466	H	N15W70	1745	M5	1660
23-06-13	8:30	21:24	339	101	S15E62	1778	M2.9	14
30-09-13	5:05	13:25	1466	H	N15W40	N/A	N/A	182
28-12-13	21:50	22:12	372	42	S18E07	1936	C9	29
06-01-14	9:15	10:24	957	76	S15E90	1936	N/A	42
06-01-14	9:15	10:24	957	76	S15W11	1944	X1	1033
07-01-14	19:55	18:24	1830	H	S15W11	1944	X1.2	1026
20-02-14	8:15	8:04	948	H	S15W73	1976	M3	22
25-02-14	3:50	1:25	2147	H	S12E62	1990	M4.9	24
18-04-14	13:40	13:31	1203	H	S20W34	2036	NM7.3	58
10-09-14	21:35	18:00	1425	H	N14E02	2158	X1.6	20
18-06-15	11:35	9:36	189	35	S13W102	2365	M1.3	16
29-10-15	5:50	2:36	530	202	NO FLARE			23
02-01-16	4:30	4:12	271	29	S21W73	2473	M2	21
05-09-17	7:51	15:42	377	47	S08W16	2673	M5	210